

Heterogeneity in Stochastic Epidemic Models

Candidate Number: 1041671



A dissertation submitted in partial fulfillment for the
degree of MSc in Mathematical Sciences.

Trinity Term, 2020

Mathematics Institute
University of Oxford

Abstract

Stochastic models in epidemiology have become increasingly popular due to their ability to better capture the inherent variability of disease propagation. The non-deterministic nature of a stochastic model means that we can consider properties like the probability of a major epidemic, which are unsuitable for classical deterministic epidemic models. In this report, we focus on how heterogeneous structures can be introduced to stochastic epidemic models, so that their dynamics are more accurate to real-world outbreaks. Specifically, we first consider extending the stochastic SIR model to include a time-heterogeneous contact rate. In addition, we produce a novel model that describes how the probability of a resulting major epidemic depends on the infective introduction time. Separately, we also consider introducing heterogeneity into a model by stratifying a population into distinct, heterogeneous types. Utilising results from spectral theory, we present a model that can be used to find which type is most responsible for a resulting epidemic. We conclude our exploration into heterogeneous model structures by considering applications motivated from current literature.

Contents

1	Introduction	3
2	Introduction to Stochastic Epidemic Models	4
2.1	The Stochastic SIR	4
2.2	Branching Process Approximation	6
2.3	Basic Reproductive Number	9
3	The Gillespie Algorithm	10
3.1	Gillespie Algorithm	10
4	Infective Introduction Time	12
4.1	An ODE Approximation	13
4.2	Time Dependent Gillespie Algorithm	14
4.2.1	Time Inhomogenous Waiting Times	14
4.2.2	Time Dependent Gillespie	15
4.3	Exponential Decay Model	16
4.4	Cosine Model	18
5	Multi-type Models and Importance	21
5.1	Next Generation Matrix	22
5.2	Dynamical Importance	25
5.3	Application	27
6	Discussion and Further Work	31

1 Introduction

Epidemiology is the study and analysis of health and disease related events that affect a specific population. The spread and control of infectious diseases is a major public health concern, with three out of the ten top causes of deaths worldwide being communicable diseases [1]. Mathematical models for infectious diseases originated with Bernoulli in the 18th century with an attempt to monitor the transmission of smallpox. More generalisable models were then developed by Ross [2], and Kermack and McKendrick [3] in the 20th century. Such models were deterministic in nature, and it wasn't until Bartlett [4] and Bailey [5] in the 1950's that the baseline stochastic models were proposed. Recently, the class of deterministic epidemic models have fallen in popularity due to the versatility of their stochastic counterparts. Stochastic epidemic models, which we will introduce shortly, are particularly popular because they better capture the inherent variability and uncertain nature of real life epidemics [6]. Stochastic models are also favoured when modelling smaller populations or single communities because of the randomness that person-to-person contact can play in the role of disease transmission. Models with stochastic dynamics can be used to answer questions unsuited to deterministic models, such as: What is the *probability* of a major epidemic? If there is such an epidemic, what is its *expected* duration? In this report, we consider extending the original stochastic models presented by Bailey by introducing heterogeneity, which allows us to encapsulate more complex infection dynamics. We also observe how the dynamics of a resulting epidemic depend on the various heterogeneous structures we implement.

This report is structured such that in Section 2, we give an introduction to a basic stochastic model (the SIR model), and present important results of such a model and how they can be obtained. We then consider how such a model can be simulated numerically using the Gillespie Algorithm within Section 3. Within Sections 4 and 5, we discuss how a heterogeneous structure can be incorporated into stochastic epidemic models and why they are needed. More specifically, in Section 4 we provide a novel model that observes the effect a time-dependent contact rate has on the probability of a resulting epidemic. In Section 5, we describe how an age-stratified, heterogeneous population can be modelled, and provide a novel application of theory from network science to find which members of a population are most important to the spread of an epidemic. We note that all figures and numerical examples are explicitly provided by the author, and displayed in an anonymous code repository, which we encourage the reader to view [7].

2 Introduction to Stochastic Epidemic Models

In this report, we limit our discussion of epidemics to the class of stochastic models, originally proposed by Bailey and Bartlett. To aide in the explanation of certain models, we may also present their deterministic counterparts, however we do not provide an introduction to such models, and instead refer the reader to the vast amount of literature on the topic [8], [9]. The pre-determined nature of deterministic models mean that they fail to capture the randomness of disease propagation. For communicable disease models, such as those considered in this report, the propagation of an infection depends entirely on contacts between members of a population. In populations like humans, these contacts occur randomly, meaning that the number of infected individuals at any point in time has intrinsic variability (and cannot be written in closed form solution). By modelling the spread of infection as a random process, stochastic models were developed to better capture these unpredictable dynamics.

Stochastic models formulate the spread of infection between infectious individuals (which we label *infectives*) and healthy individuals (referred to as *susceptibles*), through some form of transmission channel or contact. Upon infection, a susceptible undergoes a transition to become an infective; typically, such a transition is assumed to be instant, however a latent period may be introduced to provide a more accurate transition stage (explored further in [10]). In this chapter, we motivate the class of stochastic epidemic models through a basic example, called the SIR model, before discussing how we can infer properties of such a model through various approximations.

2.1 The Stochastic SIR

The stochastic SIR model, first introduced by Bailey in 1950 [5], is a model for a population split into three types, consisting of susceptibles, infectives and removals (hence the abbreviation SIR). A removed individual is one who, after being infective, can no longer infect or be re-infected (for example due to recovery and subsequent immunity, or death). A removed individual is also referred to as a recovered individual within the literature, to emphasise the fact they have previously been infected and are now immune. In addition

to dividing the population into three types, we also consider the population to be closed, meaning that if we let the triple $(S, I, R)(t)$ denote the number of susceptible, infective and removed individuals in the system at time t , then

$$S(t) + I(t) + R(t) = N, \quad N \in \mathbb{R} \quad (1)$$

for all time $t > 0$. To understand how the quantities $(S, I, R)(t)$ change during an epidemic, we need to mathematically formulate how a susceptible transitions to an infective (through disease transmission) and how a infective becomes a removed individual. Suppose that our closed population is heterogeneously mixed, meaning that every individual has equal probability of coming into contact with one another, and that a single individual makes β contacts per unit of time. The rate of contacts between a single susceptible and all infectives at time t is therefore $\beta \frac{I(t)}{N}$, where $\frac{I(t)}{N}$ is the fraction of infectives in the population. Noting that there are $S(t)$ susceptibles in the population at time t , the total rate of contacts between susceptibles and infectives (and therefore the rate of new infections) is thus $\frac{\beta}{N} S(t) I(t)$. In addition to modelling the transmission of infections, we must also consider how an infective individual transitions to a removed state. If a single infective transitions to a removal with rate γ , then the total rate of recoveries in the system at time t is given by $\gamma I(t)$. These infection and removal rates are identical to the formulation of the analogous deterministic SIR model, by Kermack and McKendrick [3], which can be written as a system of ordinary differential equations (ODEs),

$$\begin{aligned} \frac{dS}{dt} &= -\frac{\beta}{N} SI, \\ \frac{dI}{dt} &= \frac{\beta}{N} SI - \gamma I, \\ \frac{dR}{dt} &= \gamma I. \end{aligned}$$

Now that we have mathematically defined how the events within our SIR system occur, we can subsequently consider how an epidemic propagates, based upon the infection of susceptibles and the removal of infectives. To model the spread of an infection, we consider the triple $(S, I, R)(t)$ to be a Continuous Time Markov Chain (CTMC). That is, we model our population on a continuous time scale $t \in [0, \infty)$ with states $S(t), I(t), R(t) \in \{0, 1, 2, \dots, N\}$ (in addition to imposing the population condition given by (1)). We close the

CTMC model by specifying its initial conditions, that is we consider introducing a initial infectives to an otherwise fully susceptible population such that $(S, I, R)(0) = (N-a, a, 0)$. Due to the fact that the population is closed for all time, we can choose to only track two sub-populations (the third can be easily deducted using (1)), which we choose to be $S(t)$ and $I(t)$. This reduces our CTMC model to a time homogeneous bivariate Markov process $\{(S, I)(t) : t \geq 0\}$. To observe the temporal dynamics of this process (how an infection spreads through a population), we first consider how it develops in an infinitesimal time period. That is, we consider the evolution of the process $\{(S, I)(t) : t \geq 0\}$ in the interval $[t, t + \delta t)$, where δt is small enough such that a maximum of one event (an infection or a removal) can occur in the system. The infinitesimal transition probabilities of the Markov process can then be defined as follows

$$\begin{aligned}\mathbb{P}\{(S, I)(t + \delta t) = (i - 1, j + 1) \mid (S, I)(t) = (i, j)\} &= \frac{\beta}{N}ij\delta t + o(\delta t) \\ \mathbb{P}\{(S, I)(t + \delta t) = (i, j - 1) \mid (S, I)(t) = (i, j)\} &= \gamma j\delta t + o(\delta t) \\ \mathbb{P}\{(S, I)(t + \delta t) = (i, j) \mid (S, I)(t) = (i, j)\} &= 1 - (\frac{\beta}{N}ij + \gamma j)\delta t + o(\delta t)\end{aligned}\tag{2}$$

where β again denotes the average number of contacts in the system (also called the pairwise infection parameter) and γ denotes the removal rate. The first two transition probabilities correspond to an infection and removal occurring respectively, whilst the last line denotes the probability that no event occurs in the interval $[t, t + \delta t)$.

2.2 Branching Process Approximation

With stochastic epidemic models, we are often interested in answering questions such as: what is the *probability* of an epidemic occurring? What is it's expected duration and what is the variance of this quantity? As we have previously described, such questions can only be answered by stochastic models (rather than their deterministic analogue), as they can capture the inherent randomness of disease transmission. Although stochastic models of epidemics are intuitively more applicable, they have one major drawback, which is the lack of analytical tractability. Since there exists no closed solution for general stochastic models, the dynamics of any particular model cannot be interpreted directly. Instead, properties of the dynamics must

either be approximated analytically or derived from numerical simulations. A popular approximation for a stochastic model, which can be used to find the probability of a resulting epidemic as we will now show, is to consider it's dynamics as a branching process. To formally consider the probability of a resulting epidemic, we must first mathematically define what it means for an epidemic to occur. Intuitively we know what an epidemic is (we got this far in the report without having defined it), but to give it a precise definition is ambiguous. Within the literature, as originally posed by Whittle [11], we typically split the word epidemic into two cases, which we call major and minor epidemics. A minor epidemic is the realisation of an epidemic in which the infection is short-lived and has substantially fewer cases than the corresponding major epidemic. In this report, we define a major epidemic based on the total number of infections over the disease's history – known as its *final size*. In our practical implementations, we specify a threshold $F \in \mathbb{R}$ and classify an epidemic realisation as major if its final size is above this threshold. Alternative definitions of epidemic classifications, using the time until extinction have been proposed, and have been further explored by Thompson et al. in [12].

We simplify the dynamics of the SIR model by considering the bivariate Markov process $\{(S, I)(t) : t \geq 0\}$ as a branching process. This branching process is used to approximate the early-time behaviour of an epidemic, when the number of infectives is low and the population is almost entirely made up of susceptibles. The approximation allows us to find the probability an epidemic becomes extinct early in its lifetime (the probability an epidemic is minor rather than major). To map the SIR CTMC model defined by (2) to such a branching process, we consider a population in which a sole infective has been introduced. By assuming that the size of the population is sufficiently large (so that $N - 1 \approx N$), we consider the number of susceptibles to be constant, that is $S(t) = N$ for all $t > 0$. If we let $p_j(t)$ be the probability of j infectives at time t , then we can reduce the non-linear terms of the CTMC transition probabilities given by (2) to

$$p_k(t + \delta t) = \begin{cases} \beta j \delta t + o(\delta t), & \text{if } k = j + 1 \\ \gamma j \delta t + o(t), & \text{if } k = j - 1 \\ 1 - (\beta j \delta t + \gamma j \delta t) + o(\delta t), & \text{if } k = j \\ o(\delta t), & \text{otherwise.} \end{cases} \quad (3)$$

By linearizing the dynamics of the model, we have reduced the bivariate process to a branching process tracking only the number of infectives (more specifically, a Galton-Watson process with linear birth and death rates [13]). Unlike CTMC models, branching processes have properties that can be studied analytically; in particular, we can easily find the probability of extinction for a branching process (which we equate to the probability of no major epidemic in the corresponding full epidemic model). We do so by considering the probability generating function (PGF) for the offspring of a single infective in an infinitesimal time interval. If we let X be a random variable denoting the number of infected offspring produced by a single infective in a fully susceptible population, then the PGF G for X , which takes the general form

$$G(s) = \sum_{k=-\infty}^{\infty} \mathbb{P}(X = k) s^k,$$

can be written as

$$G(s) = \frac{\gamma}{\gamma + \beta} + \frac{\beta}{\gamma + \beta} s^2. \quad (4)$$

The first term of (4), corresponds to the relative probability of a removal and hence $X = 0$ offspring occurring. Meanwhile the second term denotes the probability of an infection occurring in the system and hence $X = 2$ offspring (the parent and the new infective). Unlike typical discrete-time branching processes (such as the Reed-Frost model [14]), in which the offspring of an individual replaces the parent, in the continuous time model the parent and offspring can co-exist. Here we have also implicitly applied an assumption of heterogeneous mixing within the population as well as independence between the behaviour of the two infected individuals. It is well known in the study of branching processes, that the probability of extinction for such a process is given by the smallest root of $s = G(s)$ [15]. Applying this to the PGF for our SIR branching process, we find that the probability of extinction, and thus the probability of no major epidemic, which we denote by q , is given by

$$q = \min \left\{ \frac{\gamma}{\beta}, 1 \right\}. \quad (5)$$

2.3 Basic Reproductive Number

The probability of no major epidemic can be interpreted to have an epidemiological meaning, which is given in terms of the basic reproductive number. The basic reproductive number \mathcal{R}_0 for a simple model, is described as the expected number of infections produced by a single infective in a completely susceptible population. In a wholly susceptible population with one infective, infectious contacts occur with rate β . The number of contacts over an infective's lifetime is therefore the rate of contacts multiplied by the expected time an infective is infectious, which is given by $\frac{1}{\gamma}$. Thus, the basic reproduction number for the stochastic SIR model is

$$\mathcal{R}_0 = \frac{\beta}{\gamma}.$$

From (5), we see that if $\mathcal{R}_0 < 1$, the contact rate is lower than the removal rate and no major epidemic occurs. Conversely if $\mathcal{R}_0 > 1$, when contacts occur more frequently than removals, there is a non-zero probability that the epidemic grows unbounded initially. In Figure 1, we compare the probability of no major epidemic using the analytical branching process approximation with that of numerical simulations of our CTMC model. In the next section, we discuss how these numerical simulations can be obtained and used to further explore the dynamics of a stochastic epidemic model.

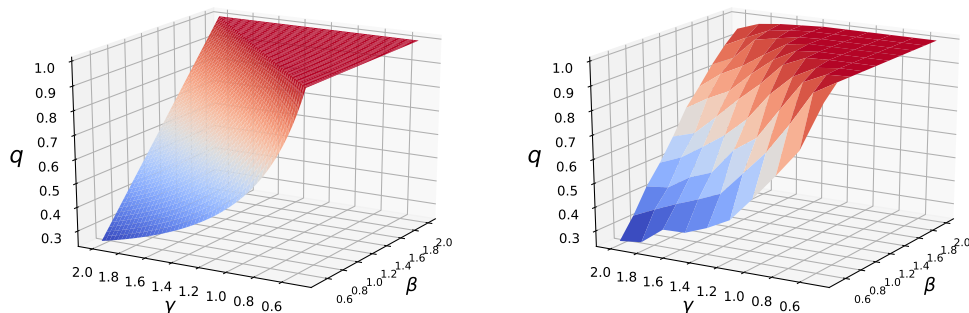


Figure 1: Left: We plot the probability of no major epidemic, given by the branching process approximation (5). **Right:** We plot the probability of no major epidemic from numerical simulations, where for each (β, γ) pair we run 1000 simulations for a population of 5000 individuals. We classify an epidemic as major if its final size was above $F = 150$.

3 The Gillespie Algorithm

The stochastic nature of CTMC models means that certain properties of their dynamics are intractable via direct calculation or analytical approximations; an example of such a property is the bi-modal distribution of the time to extinction [16] (which is explored separately by the author in [7]). Instead, one can approximate these properties by numerically simulating many realisations of the CTMC model. A popular method for the simulation of CTMC models is the Gillespie algorithm [17], which we will now present.

3.1 Gillespie Algorithm

We start by presenting the Gillespie algorithm in a general setting, before relating it back to its use in modelling the SIR model presented in Section 2.1. Suppose that in our system, there are N species represented by $Y = (X_1, X_2, \dots, X_N)$, which may react through M different reaction channels. Each reaction R_μ occurs according to an infinitesimal probability, which we call its propensity function a_μ . That is, in the interval $[t, t + \delta t)$, the reaction R_μ occurs with probability $a_\mu \delta t + o(\delta t)$. To each reaction, we also assume a stoichiometric vector v_μ , which defines the change in the state of the system Y based on the reaction R_μ occurring.

To simulate a system defined under the reactions R_μ , $\mu \in \{1, \dots, M\}$, we split the simulation problem into two sections. We must first find the time at which the next reaction occurs. After finding this time, we need decide which reaction of the M reactions occurs at this point. The Gillespie algorithm proposes efficient methods of calculating both of these quantities, using the fact that reactions are independent and that a single reaction μ is distributed according to a Poisson process with rate a_μ . We explore these facts further in Section 4.2.1, when we extend the Gillespie algorithm to more complex dynamics.

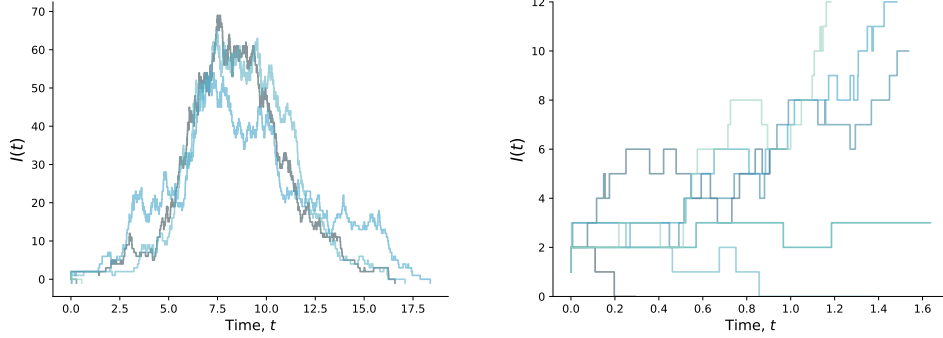


Figure 2: Eight stochastic simulations of the SIR model with parameter values $\beta = 2$, $\gamma = 1$; the initial conditions of the system were $(S, I, R)(0) = (499, 1, 0)$. **Left:** Figure displays entire dynamics of eight realisations. **Right:** Figure displays their dynamics shortly after the introduction of an infective. See [7] for numerical implementation.

Algorithm 1 Direct Gillespie Algorithm

- 1: Start the algorithm at $t = 0$
- 2: Specify $Y(0) = (X_1, X_2, \dots, X_N)(0)$ and propensities (a_1, a_2, \dots, a_M) .
- 3: Compute $a_0 = \sum_{\mu=1}^M a_\mu$.
- 4: Generate two uniformly random numbers $u_1, u_2 \sim \text{Uniform}(0, 1)$.
- 5: Compute next reaction time, $t + \tau$ where

$$\tau = \frac{1}{a_0} \log \left(\frac{1}{u_1} \right)$$

- 6: Find integer ν such that $\sum_{\mu=1}^{\nu-1} a_\mu < u_2 a_0 \leq \sum_{\mu=1}^{\nu} a_\mu$
 - 7: Update system based on reaction ν firing; $Y(t + \tau) = Y(t) + v_\nu$
 - 8: Evaluate termination criteria
 - 9: If pass, set $t = t + \tau$ and proceed to Step 3.
 - 10: Else, exit the algorithm.
-

In the application to our stochastic SIR model, we have two propensity functions, namely $a_1 = \frac{\beta}{N} S(t)I(t)$ and $a_2 = \gamma I(t)$ which have corresponding stoichiometric vectors $v_1 = (-1, +1, 0)^T$ and $v_2 = (0, -1, +1)^T$. The termination criteria for the algorithm to end is simply if $I(t)$ has hit zero; if it has, then the epidemic has ended and we no longer need to model the population.

4 Infective Introduction Time

In this chapter, we will present a novel model that can be used to approximate how the probability of a major epidemic depends on the time that an infective was introduced to a population. This is of importance in more complex epidemic models, like those we will now consider, where the contact rate between individuals has time dependence. So far, we have only considered models with a constant rate parameter $\beta \in \mathbb{R}$, however this is not particularly accurate in real-world applications, where the dynamics between susceptible and infectives are always changing. To more accurately model such scenarios, we define a new time inhomogeneous CTMC model, which we build from the basic stochastic SIR model described in Section 2.1. We again model the number of susceptibles and infectives as a bivariate Markov process $\{(S, I)(t) : t \geq 0\}$, except now we have the following infinitesimal transition probabilities

$$p_{k,l}(t + \delta t) = \begin{cases} \frac{B(t)}{N}ij\delta t + o(\delta t), & \text{if } (k, l) = (i - 1, j + 1) \\ \gamma j\delta t + o(t), & \text{if } (k, l) = (i, j - 1) \\ 1 - (\frac{B(t)}{N}ij\delta t + \gamma j\delta t) + o(\delta t), & \text{if } (k, l) = (i, j) \\ o(\delta t), & \text{otherwise.} \end{cases} \quad (6)$$

The function $B(t)$ now explicitly captures how the rate of contacts a single individual makes changes in time, rather than simply being constant, as was the case previously.

We are now interested in how the probability of a major epidemic, like that of Section 2.2, differs now that our model has explicit time dependence. To observe how this time heterogeneity adds more complexity to an epidemic model, we consider the time that an infective is introduced and the effect that this has on a resulting epidemic. The motivation for this framework is clear, for example such a model would allow us to understand how the probability of a major epidemic differs when an infective is introduced in the winter to the summer. We will now present a novel ODE model for how infective introduction time effects the probability of a resulting epidemic, before applying such a model to contact rates motivated from real-world outbreaks.

4.1 An ODE Approximation

To develop our ODE model, we first simplify the dynamics of our new CTMC model, given by (6). That is, in a similar vein to Section 2.2, we consider a birth-death process in which the number of susceptibles is constant, and equal to N for all time. If we let $p_j(t)$ be the probability of j infectives at time t , then the transition probabilities of the simplified CTMC model can be written

$$p_k(t + \delta t) = \begin{cases} B(t)j\delta t + o(\delta t), & \text{if } k = j + 1 \\ \gamma j\delta t + o(t), & \text{if } k = j - 1 \\ 1 - (B(t)j\delta t + \gamma j\delta t) + o(\delta t), & \text{if } k = j \\ o(\delta t), & \text{otherwise.} \end{cases} \quad (7)$$

Now we wish to understand how the dynamics of this process differ, based upon the time \bar{t} that an infective is introduced to the system. To do so, we consider how the process develops in an infinitesimal time period. If we let $q(1, \bar{t})$ be the probability of no major epidemic, given a single infective is introduced to the population at time \bar{t} , then by the law of total probability, it satisfies

$$\begin{aligned} q(1, \bar{t}) &= B(\bar{t})q(2, \bar{t} + \delta t)\delta t \\ &\quad + \gamma q(0, \bar{t} + \delta t)\delta t. \\ &\quad + (1 - B(\bar{t})\delta t - \gamma\delta t)q(1, \bar{t} + \delta t) \end{aligned} \quad (8)$$

Where the first, second and third term of the right-hand side correspond to an infection, removal and no event occurring respectively, within the infinitesimal time period $[\bar{t}, \bar{t} + \delta t)$. More explicitly, if an infection occurs within this interval, then at time $\bar{t} + \delta t$ there will now be two infective individuals in the system and thus the probability of no major epidemic originally given by $q(1, \bar{t})$ becomes $q(2, \bar{t} + \delta t)$, conditioned on an infection occurring. If instead a removal occurs, then the probability of no major epidemic becomes $q(0, \bar{t} + \delta t)$ which we note is equal to one (since the only infective in the system has been removed, meaning no major epidemic can occur). The final term corresponds to the probability of no major epidemic given that no event occurs, which is simply $q(1, \bar{t} + \delta t)$. We can further simplify (8) by employing a branching process approximation; if the population is sufficiently large and homogeneously mixed, then we can consider the lineages of two infective

individuals to be independent. This means that $q(2, \bar{t} + \delta t) = q(1, \bar{t} + \delta t)^2$, the probability of extinction for two infectives is equal to two single infective lineages going extinct independently. Re-arranging (8) and taking the limit as $\delta t \rightarrow 0$, we obtain

$$\frac{dq(\bar{t})}{d\bar{t}} = -B(\bar{t})q^2 + (B(\bar{t}) + \gamma)q - \gamma \quad (9)$$

where we have omitted the first variable of q since it is equal to one for all the terms. The general solution of such an ODE can be written as

$$q(\bar{t}) = 1 - \frac{\exp\{-\int^{\bar{t}} (B(t') - \gamma) dt'\}}{C - \int^{\bar{t}} B(t') \exp\{-\int^{t'} (B(\tau) - \gamma) d\tau\} dt'}. \quad (10)$$

The derivation of the general solution is outlined in Appendix A. To find the integration constant $C \in \mathbb{R}$, one can apply several techniques; firstly one can assume properties of the function $q(\bar{t})$, for example if it is 2π -periodic. Another way to find the integration constant is by using numerical simulations, introducing the initial infective at time $\bar{t} = 0$.

4.2 Time Dependent Gillespie Algorithm

To simulate the dynamics of a time-heterogeneous CTMC model, we need to alter the Gillespie algorithm presented in Section 3 since the propensity functions $a_\mu(t)$ have explicit time dependence. Instead of a reaction μ occurring according to a standard Poisson process, as was the case previously, it now fires according to a time dependent Poisson process (described at more detail in [18]).

4.2.1 Time Inhomogenous Waiting Times

One now models the reaction R_μ as a time inhomogeneous Poisson process $\{P_\mu(t) : t \geq 0\}$, where P_μ counts the number of times reaction μ occurs. Using the infinitesimal probability of the reaction R_μ firing from Section 3, we have that

$$\begin{aligned} \mathbb{P}\{P_\mu(t + \delta t) - P_\mu(t) = 0\} &= 1 - a_\mu(t)\delta t + o(\delta t) \\ \mathbb{P}\{P_\mu(t + \delta t) - P_\mu(t) = 1\} &= a_\mu(t)\delta t + o(\delta t) \\ \mathbb{P}\{P_\mu(t + \delta t) - P_\mu(t) \geq 1\} &= o(\delta t). \end{aligned}$$

The probability mass function of such a Poisson process P_μ can be written

$$\mathbb{P}(P_\mu(t) = k) = \frac{(A_\mu(t))^k e^{-A_\mu(t)}}{k!}, \text{ where } A_\mu(t) = \int_0^t a_\mu(s) ds. \quad (11)$$

As was the case for the standard Gillespie algorithm, we wish to find the time in which a reaction μ occurs next. The distribution of such a waiting time, denoted by T_μ , can be found by using the Poisson process defined above,

$$\begin{aligned} \mathbb{P}(T_\mu > t) &= \mathbb{P}(P_\mu(t) = 0) = \exp \left\{ - \int_0^t a_\mu(s) ds \right\}, \text{ therefore} \\ \mathbb{P}(T_\mu < t) &= 1 - \exp \left\{ - \int_0^t a_\mu(s) ds \right\}. \end{aligned}$$

Thus, the waiting time for the reaction R_μ to occur is exponentially distributed with rate $1/\int_0^t a_\mu(s) ds$. Since the firing of all the reactions $\mu = 1, 2, \dots, M$ are independent, the waiting time τ for any one of the reactions to occur is exponentially distributed with the following cumulative density function

$$\mathbb{P}(\tau < t) = 1 - \exp \left\{ - \int_0^t \sum_{\mu=1}^M a_\mu(s) ds \right\}. \quad (12)$$

4.2.2 Time Dependent Gillespie

By utilizing the distribution of the waiting time for our system, given by (12), we can adapt Algorithm 1 to handle time-dependent propensity functions. To generate the next reaction time, given that the system is currently at time $\bar{\tau}$ we employ the inversion method from simulation theory [18]; that is if we generate u , a number uniformly distributed on the interval $[0, 1]$, then the waiting time until the next reaction of the system Δt is a zero of the following generally non-linear function

$$f(\Delta t) = \int_{\bar{\tau}}^{\bar{\tau} + \Delta t} \sum_{\mu=1}^M a_\mu(s) ds - \log(1 - u). \quad (13)$$

For propensities that have well defined integrals, this equation can be solved by employing a non-linear equation solver. In this report, we use a Python implementation of a Broyden solver to obtain the zero of f if it cannot

be obtained analytically [19]. To find which reaction occurs at the next reaction time, one can simply use the method of vanilla Gillespie. That is, the probability of selecting a particular reaction is proportional to its propensity function at the new reaction time. Since we are now able to find when the next reaction will occur and which reaction it will be, we can consider an adapted variant of Algorithm 1, for temporal propensity functions.

Algorithm 2 Temporal Gillespie Algorithm

- 1: Start the algorithm at a specified time $t = \bar{t}$
- 2: Specify $Y(\bar{t}) = (X_1, X_2, \dots, X_N)(\bar{t})$ and propensities $(a_1, a_2, \dots, a_M)(t)$.
- 3: Generate two uniformly random numbers $u_1, u_2 \sim \text{Uniform}(0, 1)$.
- 4: Compute next reaction time, by finding Δt such that

$$\int_t^{t+\Delta t} \sum_{\mu=1}^M a_{\mu}(s) ds - \log(1 - u_1) = 0$$

- 5: Find integer ν such that

$$\sum_{\mu=1}^{\nu-1} a_{\mu}(t + \Delta t) < u_2 \sum_{\mu=1}^M a_{\mu}(t + \Delta t) \leq \sum_{\mu=1}^{\nu} a_{\mu}(t + \Delta t)$$

- 6: Update system based on reaction ν firing; $Y(t + \tau) = Y(t) + v_{\nu}$
 - 7: Evaluate termination criteria:
 - 8: If pass, set $t = t + \Delta t$ and proceed to Step 3.
 - 9: Else, exit the algorithm.
-

4.3 Exponential Decay Model

In this section and the following, we apply the results of this chapter, namely (10), to different contact rate functions. We wish to observe how the probability of a (major) epidemic, given by $p(\bar{t}) = 1 - q(\bar{t})$, depends on the infective introduction time. We start by applying our ODE model to a population in which contacts are exponentially decaying in time, that is the contact rate takes the form

$$B(t; A, D, \alpha) = D + Ae^{-\alpha t}, \quad (14)$$

for parameters A , D and α . This type of contact rate has been proposed previously, namely by Chowell et al. [20]. In such literature, the contact rate was motivated by how international medical intervention and disease control can reduce the number of infective contacts in future disease outbreaks. In particular, they were concerned with how the \mathcal{R}_0 changed from 1995 when an Ebola epidemic occurred in the Congo compared to the latter outbreak in Uganda (2000). Using our ODE model, we can observe the influence of the intervention on the probability of a major epidemic occurring. For example, suppose that there was a single infective introduced into a neighbouring country of the Congo any time between 1995 and 2000, then we can use (10) to observe the effect that the intervention had on the probability of an epidemic occurring in that country. In Figure 3, we plot the probability of a major epidemic (found by taking $1 - q(\bar{t})$), which can be written as

$$p(\bar{t}) = \frac{\exp\left\{(\gamma - D)\bar{t} + \frac{A}{\alpha}e^{-\alpha\bar{t}}\right\}}{C - \int^{\bar{t}} (D + Ae^{-\alpha t'}) \exp\left\{(\gamma - D)t' + \frac{A}{\alpha}e^{-\alpha t'}\right\} dt'}. \quad (15)$$

We compare our ODE approximation against results from numerical simulations of the CTMC model, using parameters $D = 0.8$, $A = 1.3$, $\alpha = 0.2$ and removal rate $\gamma = 1$. These parameter values were chosen so that the contact rate initially starts higher than the removal rate before becoming lower with sufficient time. We note that in the simulations of such a model, the waiting time can be found simply by using solutions of the Lambert function, this is discussed more explicitly in our practical implementation [7]. We also compare our ODE solution and simulations to what we refer to as the instantaneous probability, given by

$$\text{instantaneous probability: } 1 - \min\left\{\frac{\gamma}{B(\bar{t})}, 1\right\}, \quad (16)$$

where \bar{t} denotes the infective introduction time. This gives the probability of a major epidemic, when we assume that upon the introduction of an infective to the system, the contact rate will remain constant (using the results of Section 2.2). By comparing the instantaneous rate with our novel model, we can observe the effect future changes in infection dynamics have on the probability of a resulting epidemic. In Figure 3 we observe that the instantaneous rate overestimated the probability of a major epidemic, since it does not take into account the fact that the rate of contacts will

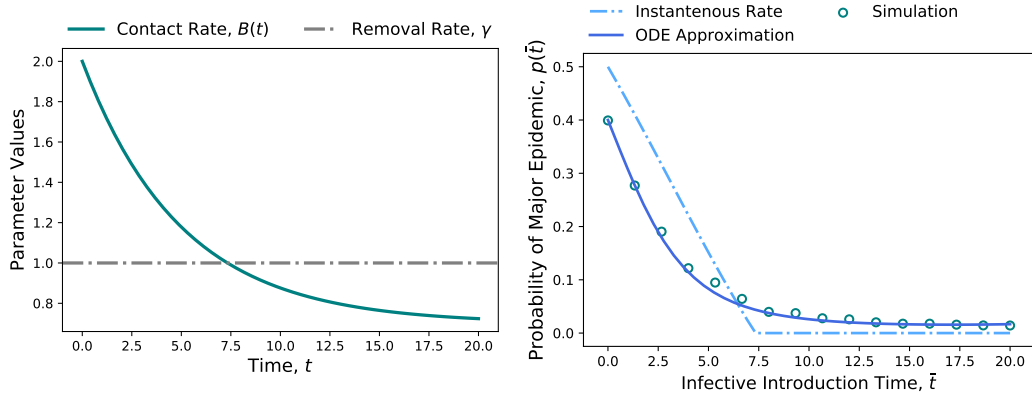


Figure 3: Left: Time dependent exponential contact rate, given by (14), with parameters $D = 0.8$, $A = 1.3$, $\alpha = 0.2$ and removal rate $\gamma = 1$. **Right:** Plots of the ODE model (15), the instantaneous probability and simulations from using the Temporal Gillespie Algorithm. The initial conditions of the system were $(S, I, R)(0) = (4999, 1, 0)$. A simulation is classified as a major epidemic if final size is larger than 50. For our ODE solution, we specify the initial condition as 0.4 (first simulation value). See [7] for implementation.

be significantly lower in the future, supporting the belief that the continued disease control in the Congo and surrounding areas had a significant impact on reducing later outbreaks [20].

4.4 Cosine Model

In addition to the exponential model discussed in the previous section, we will also apply (10) to a cyclical contact rate, which is of the form

$$B(t; A, \alpha) = A + \alpha \cos(t). \quad (17)$$

This type of contact rate function is motivated primarily from seasonal variation in population dynamics. For example in the modelling of childhood diseases such as measles [21], we see that children in primary and secondary school experience a high rate of contacts to other children during term times, and a relatively lower rate outside of these times. We can naturally use our infective introduction time model, to establish the difference between the probability of an epidemic occurring when an infective is introduced during term time, compared to the holiday period.

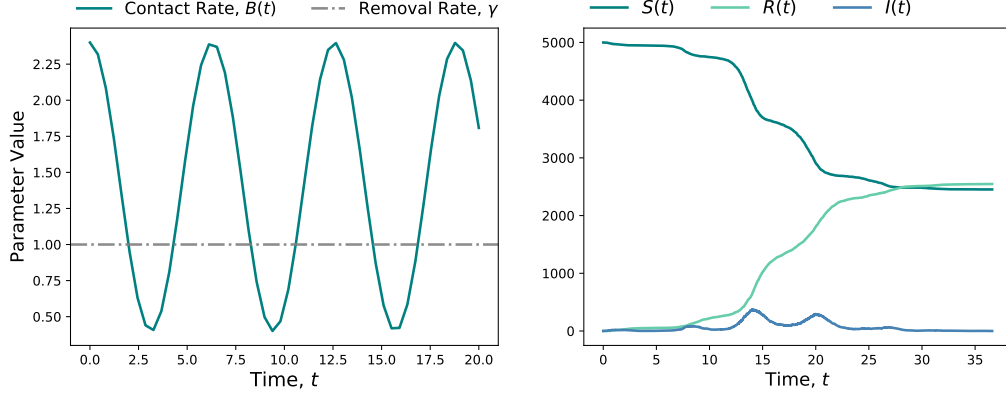


Figure 4: Left: Plots of the contact rate function $B(t)$ (17) with parameters $A = 1.4$, $\alpha = 1$ and the constant removal rate $\gamma = 1$. **Right:** Sample realisation of the CTMC model with the same contact rate and removal parameters. Simulations performed using the Temporal Gillespie Algorithm for a population with initial conditions $(S, I, R)(0) = (4999, 1, 0)$.

By applying (17) to the general solution, given by (10), we obtain the probability of a resulting major epidemic, given that an infective is introduced at time \bar{t} , as

$$p(\bar{t}) = \frac{\exp\{(\gamma - A)\bar{t} - \alpha \sin(\bar{t})\}}{C - \int^{\bar{t}} (A + \alpha \cos(t')) \exp\{(\gamma - A)t' - \alpha \sin(t')\} dt'}. \quad (18)$$

Unfortunately, the integral in the above equation is intractable and so numerical approximations must be used to obtain a solution. To eliminate the integration constant for the general solution, we assume that since the contact rate is 2π -periodic, then so must $p(\bar{t})$.

In Figure 5, we plot $p(\bar{t})$, found via MATLAB's `ode45` function, against simulations obtained by the Temporal Gillespie Algorithm. We again compare our solution to that of the instantaneous probability solution, given by

$$1 - \min\left\{\frac{\gamma}{A + \alpha \cos(\bar{t})}, 1\right\}.$$

Our novel model $p(\bar{t})$, which matches the simulations very closely, shows that the instantaneous rate both underestimates and overestimates the extrema of the probability of an epidemic. By observing Figure 5, we highlight the importance of understanding how the population dynamics may change in

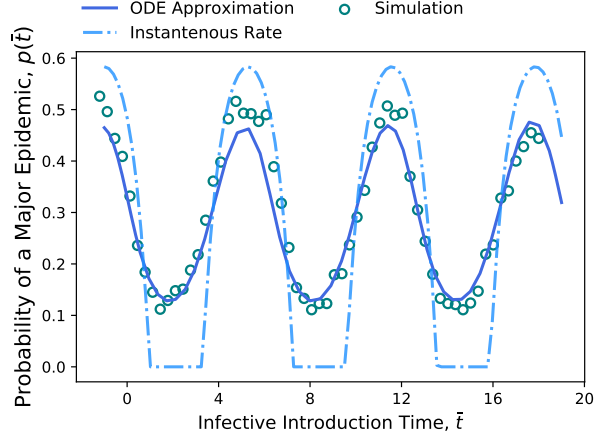


Figure 5: Plotting our ODE model (18), solved with MATLAB’s `ode45` function, against simulation results and the instantaneous probability for an epidemic with a cyclical contact rate. The initial conditions of the system were $(S, I, R)(0) = (4999, 1, 0)$, with contact rate parameters $A = 1.4, B = 1$ and constant removal rate $\gamma = 1$. A simulation is classified as a major epidemic if final size is larger than 50. We find the initial condition $p(0) \approx 0.4775$ of the ODE by assuming the function is 2π periodic. See [7] for implementation.

the future. For example, there are points at which the instantaneous model believes that there is no chance of a major epidemic when in reality, as predicted by our model, it stands at a non-negligible 15%. Thus, we may underestimate the probability of a resulting major epidemic if we do not take into account how the contact dynamics of a population may change in the near future, which could have catastrophic effects when applied to real-world outbreaks. The temporal heterogeneity we have introduced by considering time-dependent contact rates allows us to more accurately predict the probability of a major epidemic when we have non-constant contact dynamics.

5 Multi-type Models and Importance

In this latter part of the report, we shift our focus from time dependent contact rates and temporal heterogeneity to discuss multi-type models, and how they can be used to add more realism or detail to epidemic models. A multi-type SIR model is a compartmental model similar to the basic stochastic SIR model described in Section 2.1, except now we consider stratifying the population into sub-populations, which we call types. Each type is then further divided into susceptible, infective and removed states. The dynamics of a multi-type model differ from considering an SIR model for each type separately, as we allow for contact between the different types; certain models also allow for transitions between types, such as [22], however we do not consider that case here. The general form of a multi-type SIR model can be written in the following deterministic form

$$\frac{dS_i}{dt} = - \sum_{j=1}^M \frac{B_{i,j}}{N_i} S_i I_j \quad (19)$$

$$\frac{dI_i}{dt} = \sum_{j=1}^M \frac{B_{i,j}}{N_i} S_i I_j - \gamma_i I_i \quad (20)$$

$$\frac{dR_i}{dt} = \gamma_i I_i \quad (21)$$

where M is the number of types in the population and the triple (S_k, I_k, R_k) denotes the number of susceptibles, infectives and removals of type k in the system. The term $B_{i,j}$ represents the (constant) infectious contact rate between susceptibles of type i to infectives of type j . In this model, we assume a constant total population size as well as a constant type population size, meaning that $\sum_{i=1}^M N_i = N$, where $N \in \mathbb{R}$ is the total population and $S_k(t) + I_k(t) + R_k(t) = N_k \in \mathbb{R}$ is the population size for the specific type k . There are many possible motivations for utilising a multi-type SIR model to model an epidemic, all of which rely on wanting to explicitly model the heterogeneity between the members of a population. For example, one could model the spread of a sexually transmitted disease in heterosexual partners by using $M = 2$ types, with heterogeneous contact rates – a model similar to this description was considered in [23]. Later in this report, as motivated by the work of [24], we consider introducing heterogeneity by dividing a population into distinct age ranges.

The analogous stochastic CTMC model to (19)-(21) is one where we model the spread of infection as a multivariate Markov process

$$\{(S_k, I_k)(t) : k \in \{1, \dots, M\}, t > 0\}$$

with $2M$ states. We can define the transition probabilities in an infinitesimal time period for all reactions, as given in Table 1; we present these in tabular form, as writing out the dynamics in the form of (6) would be cumbersome since there are now $M(M + 1)$ possible reactions.

Table 1: Infinitesimal transition probabilities of a multi-type SIR model.

Reaction	Transition Probability
$S_i + I_j \rightarrow I_i + I_j$	$\frac{1}{N_i} B_{i,j} S_i I_j \delta t + o(\delta t)$
$I_i \rightarrow R_i$	$\gamma_i I_i \delta t + o(\delta t)$

5.1 Next Generation Matrix

An important quantity that qualitatively describes the dynamics of any epidemic model is the basic reproductive number, \mathcal{R}_0 . However, since we now have many different groups of infectious individuals, the definition of \mathcal{R}_0 from Section 2.3 is not longer applicable. To extend the definition of \mathcal{R}_0 for a population in which there are multiple infective groups, we consider the model's *next generation matrix*. The next generation matrix $\mathbf{K} \in \mathbb{R}^{M \times M}$, and its use to calculate a model's \mathcal{R}_0 was first introduced by Diekmann, in 1990 [25]. After constructing the next generation matrix, which we will now describe, one can find the system's basic reproductive number by calculating this matrix's spectral radius. To derive the next generation matrix for our specific stochastic model, one first considers linearizing the model's analogous deterministic equations, given by (19)-(21). As we have done several times already, we consider a population which is made up almost entirely of susceptibles, that is $S_k \approx N_k$ for all types $k \in \{1, \dots, M\}$. Such an approximation allows one to obtain a set of ODEs that are linear in the terms I_k . After linearizing (19)-(21), we consider a sub-system of the ODE equations called the infectious sub-system. The infectious sub-system of a model is an ODE system that describes only the dynamics of the states that are directly

responsible for infections. In our particular example of a multi-type SIR, the linearized infectious sub-system can be written as

$$\frac{dI_i}{dt} = \sum_{j=0}^M B_{i,j} I_j - \gamma_i I_i \quad \text{for } i \in \{1, 2, \dots, M\}. \quad (22)$$

Since we are now dealing with a linear ODE system, its dynamics can be written more succinctly in matrix form. If we let $I = (I_1, I_2, \dots, I_M)^T$ be the vector of infective types, then

$$\frac{dI}{dt} = \mathbf{J}I \quad (23)$$

where

$$\mathbf{J} = \begin{bmatrix} B_{1,1} - \gamma_1 & B_{1,2} & \dots & B_{1,M} \\ B_{2,1} & B_{2,2} - \gamma_2 & \dots & B_{2,M} \\ \vdots & & \ddots & \vdots \\ B_{M,1} & \dots & & B_{M,M} - \gamma_M \end{bmatrix}. \quad (24)$$

We now consider decomposing the Jacobian $\mathbf{J} \in \mathbb{R}^{M \times M}$ into the sum of two matrices, \mathbf{F} and \mathbf{V} . The matrix \mathbf{F} corresponds to the terms of \mathbf{J} that describe the transmission of infection, whilst \mathbf{V} corresponds to the remaining terms of the matrix that deal with transitions between states not due to infection, for example removals. For our model (Table 1), it is clear that

$$\mathbf{F} = \begin{bmatrix} B_{1,1} & B_{1,2} & \dots & B_{1,M} \\ B_{2,1} & B_{2,2} & \dots & B_{2,M} \\ \vdots & & \ddots & \vdots \\ B_{M,1} & \dots & & B_{M,M} \end{bmatrix} \quad \text{and} \quad \mathbf{V} = \begin{bmatrix} -\gamma_1 & 0 & \dots & 0 \\ 0 & -\gamma_2 & \ddots & \vdots \\ \vdots & \ddots & \ddots & 0 \\ 0 & \dots & 0 & -\gamma_n \end{bmatrix}.$$

From the matrices \mathbf{F} and \mathbf{V} , one can then generate the next generation matrix \mathbf{K} , via the identity

$$\mathbf{K} = -\mathbf{F}\mathbf{V}^{-1}. \quad (25)$$

We can interpret the epidemiological meaning of the next generation matrix by considering its elements $K_{i,j}$. That is $K_{i,j}$ is the expected number of new infections of type i generated during the average lifetime of an infective of type j [25]. If we consider the matrices \mathbf{F} and \mathbf{V} for our particular model,

then the corresponding next generation matrix is

$$\mathbf{K} = \begin{bmatrix} \frac{B_{1,1}}{\gamma_1} & \frac{B_{1,2}}{\gamma_2} & \cdots & \frac{B_{1,M}}{\gamma_M} \\ \frac{B_{2,1}}{\gamma_1} & \ddots & & \vdots \\ \vdots & & \ddots & \vdots \\ \frac{B_{M,1}}{\gamma_1} & \cdots & & \frac{B_{M,M}}{\gamma_M} \end{bmatrix}. \quad (26)$$

In this simple example, we can confirm the epidemiological meaning of the next generation matrix. We know from Section 4.2.1 that if the removal of an infective of type k is given by an instantaneous rate γ_k , then the expected amount of time an infective of type k stays infectious is $1/\gamma_k$. Thus the expected number of infections of type i caused by an infection of type j over its lifetime (in a fully susceptible population) is $\frac{B_{i,j}}{\gamma_j}$, the elements of \mathbf{K} .

The basic reproductive number of a system with multiple infective states is defined as the spectral radius of the next generation matrix,

$$\mathcal{R}_0 := \rho(\mathbf{K}), \text{ where } \rho(\mathbf{K}) = \max\{|\lambda_1|, |\lambda_2|, \dots, |\lambda_M|\} \quad (27)$$

and $\lambda_1, \dots, \lambda_M \in \mathbb{R}$ are the eigenvalues of \mathbf{K} . In the case of a small number of types, tractable solutions for \mathcal{R}_0 can be obtained. For example, in the case $M = 2$, Allen and Nandi [26] find the closed form solution of \mathcal{R}_0 and observe the sensitivity of \mathcal{R}_0 to certain infectivity parameters. For systems with larger numbers of types ($M \gg 2$), finding a tractable solution for \mathcal{R}_0 is incredibly cumbersome and impractical, as one has to solve the corresponding characteristic equations for \mathbf{K} . The lack of an analytical solution for \mathcal{R}_0 means that it is hard to find the sensitivity of the reproductive number to certain infectious types, contacts rates, or removal parameters. In the following section, we present a method that predicts the relative importance of a particular type, as well as a particular contact, on the spread of an epidemic.

5.2 Dynamical Importance

We are interested in observing the effect a single infectious type has on the dynamics of an epidemic model. Such a result would be important in the application of multi-type model to real world data, where we wish to find which members of a population are most responsible for a resulting epidemic. Being able to identify the population types that control the propagation of an epidemic would allow for a more robust and informed epidemic-response programme. In the following sections, we discuss how this information can be obtained, and apply it to a model that is currently very relevant in the literature, due to the ongoing pandemic of SARS-CoV-2, at the time of writing.

Analogous to the single type case, and as described in Section 2.3, the basic reproductive number for a multi-type model describes the initial dynamics of the epidemic. Re-considering the infectious subsystem given by (23), one can show that if $\mathcal{R}_0 = \rho(\mathbf{K}) < 1$ then the number of infectives decay to zero, that is the epidemic dies out before infecting more individuals. Conversely, if $\rho(\mathbf{K}) > 1$, then initially there may be exponential growth in the system and a corresponding major epidemic. The derivation of the correspondence between \mathcal{R}_0 and the dynamics of the infectious subsystem is given by Diekmann [25]. To understand how responsible a particular infective type is for a resulting epidemic, we focus on how its presence effects the initial dynamics of a CTMC model. To do so, we consider a novel application of pre-existing spectral theory to the case of stochastic epidemic models. In particular, we generate an epidemiological analogous results to that of Restrepo et al. [27], who first proposed this method for centrality measures on networks and graphs. Where they derived node and edge importance measures for the dynamics of graphs, we construct analogous results measuring the importance of a specific type and a specific contact on the dynamics of an epidemic in a multi-type SIR model. To define the type importance of a population member in the multi-type SIR model, we consider the change in the \mathcal{R}_0 between the original system, and a corresponding system where that specific type has been removed. An infectious type is therefore more important to the multi-type model, meaning that it is more responsible for a resulting epidemic, if its inclusion in the model causes a relatively larger increase in \mathcal{R}_0 .

To generate the importance measures, we start by letting λ denote the largest eigenvalue of the next-generation matrix \mathbf{K} , with corresponding left and right eigenvectors \mathbf{v} and \mathbf{u} respectively. From the Perron-Frobenius Theorem [28], since \mathbf{K} is a real square matrix with positive entries (we assume all contact rates are non-zero), then the largest eigenvalue λ is both unique and real - implying that $\mathcal{R}_0 = |\lambda|$. From [27], the dynamical importance of a type k in our population is proportional to $\Delta\lambda_k$, which represents the difference between λ and the largest eigenvalue of $\hat{\mathbf{K}}$, the next generation matrix for the system, when type k has been removed.

$$\text{Type Importance: } \mathcal{I}_k = -\frac{\Delta\lambda_k}{\lambda}. \quad (28)$$

One can also consider removing a single contact from the model, so that the infection transmission $i \rightarrow j$ is not allowed to occur (for example through quarantine measures). In this case, we can define the contact importance similarly, again using the work of [27] in a novel application. If we consider removing the contact between infectious individuals of type j and susceptibles of type i , then the dynamical importance of the the contact is given by

$$\text{Contact Importance: } \mathcal{I}_{i,j} = -\frac{\Delta\lambda_{i,j}}{\lambda}, \quad (29)$$

where $\Delta\lambda_{i,j}$ is the change in the largest eigenvalue upon the removal of the contact $B_{i,j}$ from \mathbf{K} . By removing a type or a contact entry from the elements of \mathbf{F} , we can construct a new next generation matrix $\hat{\mathbf{K}}$, which considers the system where the type or contact has been removed. In Appendix B, we show how in the case of our SIR multi-type model the results of [27] still hold, we also provide a derivation of these results, which were omitted from the original paper. The dynamical importance of a type and an infectious contact are approximated as

$$\hat{\mathcal{I}}_k = \frac{v_k u_k}{\mathbf{v}^T \mathbf{u} - v_k u_k} \quad \text{and} \quad \hat{\mathcal{I}}_{i,j} = \frac{K_{i,j} v_i u_j}{\lambda \mathbf{v}^T \mathbf{u}}. \quad (30)$$

We note that while these results have been derived using our specific multi-type SIR model as an example, the results can also be generalised to more complicated models, for example including demography. Due to the limited space of this report, such extensions are not discussed any further.

5.3 Application

In this section, we apply (28) and (29) to a multi-type model that we extend from the work of Thompson [29] on modelling the novel Coronavirus outbreak of 2019/2020. In the work of Thompson, they suggest dividing the population into two types, labelled fast and slow reporters, which we denote by R_F and R_S respectively. Fast reporters are members of the population that report their infection and seek medical attention quicker than the slow reporters. This example has been primarily motivated by the need to reduce the number of individuals infected with SARS-CoV-2. In our results, we observe that the slow reporters have a higher impact on the dynamics of an epidemic than their fast reporting counterparts and thus are more responsible for a resulting epidemic. This work suggests that relevant healthcare advertising demanding those to isolate or seek medical attention as early as possible could reduce the spread of the epidemic.

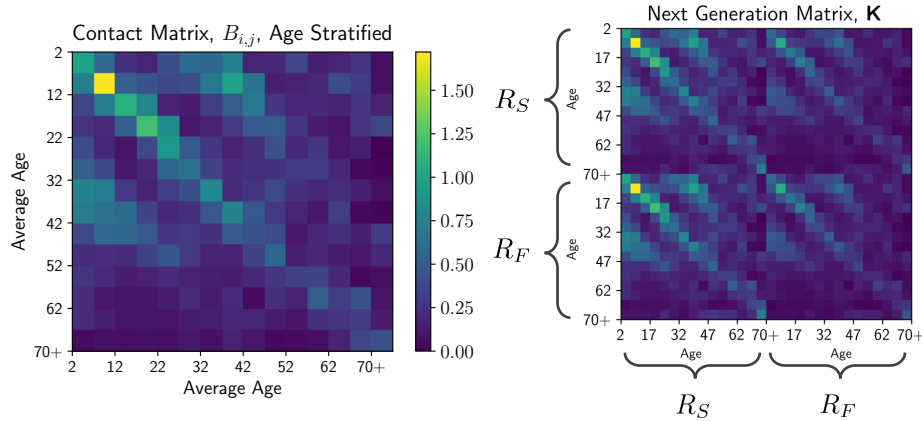


Figure 6: Left: Displaying the contact rate data for 15 age ranges from (0-4) to 70+. The data is specifically taken from Table S8.4 of [30]. **Right:** The next generation matrix, where we have $M = 30$ total types, split into fast and slow reporters, which are then further stratified by age. To separate the reporting groups, we use $\gamma_F = 0.8$ and $\gamma_S = 0.5$ for fast and slow reporters respectively.

We explore how further stratifying the fast and slow reporter populations into age groups can identify individuals most responsible for the continued transmission of an epidemic. To begin with, we stratify both reporting groups into fifteen age ranges, so that our total population contains $M = 30$ distinct types. By using data from [30] (Specifically Table S8.4 of their Supplementary Information), we obtain contact rate estimates between the age groups

within the population of the UK, displayed in Figure 6. The age-ranges we consider are 0-4, 5-9, 10-14, ..., 65-69, 70+; to simplify notation, we label these by the mid-value of the age brackets (for example, the 0-4 range is represented by the average age 2). To embed the fast and slow reporting in our model, we use the idea that was presented by Thompson in [29]; that is we give faster reporters a relatively larger recovery parameter $\gamma_F = 0.8$, compared to the slower reporters with rate $\gamma_S = 0.5$. Doing so means that the expected recovery time for a faster reporter $1/\gamma_F$ is smaller than $1/\gamma_S$. Across the age ranges of the respective reporting groups, the recovery rate is constant. For all 30 types, we consider an equal, constant type population size.

After computing the next-generation matrix \mathbf{K} (displayed in Figure 6) and applying (30) to this multi-type model, we obtain the following results for both the infectious type and contact importance, displayed in Figure 7. We see that in Figure 7 (Left) that, for all ages, the slow reporters are more important in contributing to an epidemic than their fast reporting counterparts. In particular, when we consider age brackets that are relatively more important (for example the bracket 5-9), the difference between the two reporting groups is even more significant.

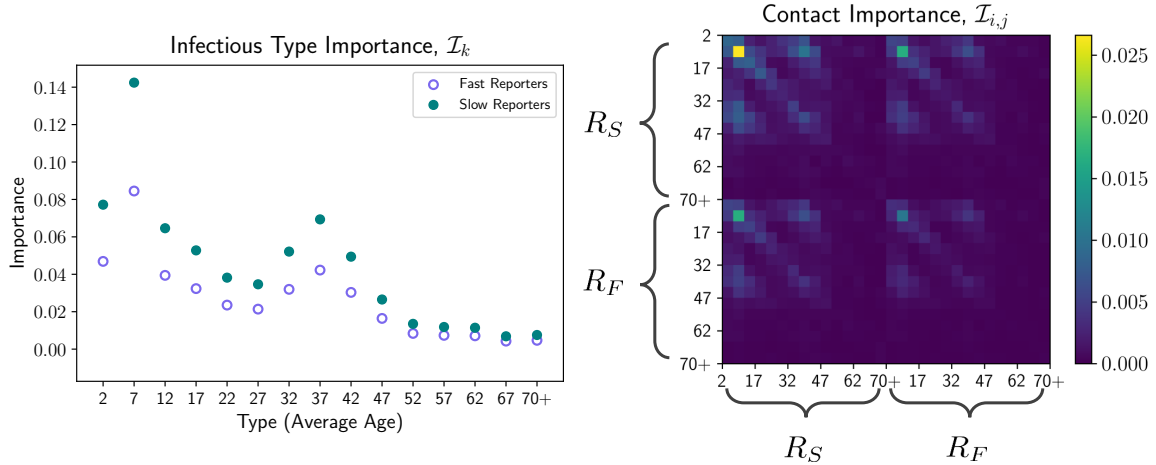


Figure 7: Left: Plotting the infectious type importance, given by (28) for our multi-type model. We split the $M = 30$ types into the fast and slow reporting groups to compare the the corresponding age-range importance. **Right:** The contact importance matrix, with entries given by (29), we label the contacts by which reporting group they belong.

Due to the high level of granularity in the data, lots of contacts are relatively less important, meaning Figure 7 (Right) is hard to interpret. We therefore also plot subsets of the contact importance matrix, displaying the importance within the fast and slow reporting groups (the upper left (R_S, R_S) and lower right (R_F, R_F) blocks of Figure 7 (Right)), for ages that have non-negligible importance values; these are displayed in Figure 8. The contact importance matrix $\hat{\mathcal{I}}_{i,j}$ shares a similar result to the type importance. From observing Figure 8 further, we see that the within-group contacts of the slow reporting group R_S have a higher importance than that of the contacts for types in the fast reporting group R_F .

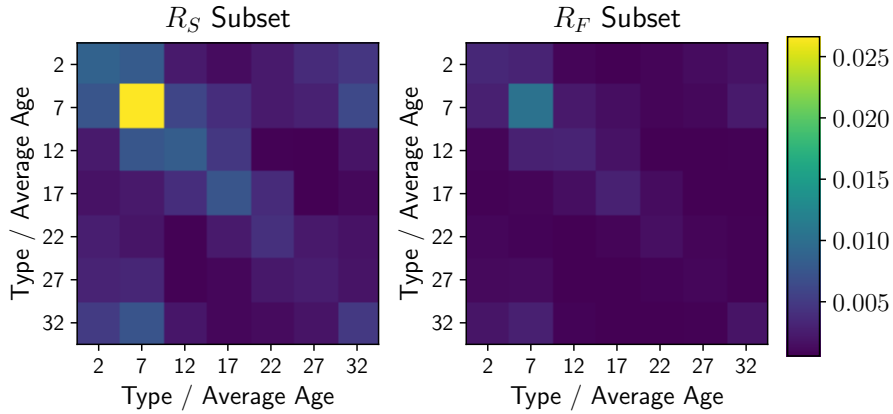


Figure 8: A plot of the the importance matrix given in Figure 7 (Right), where we compare the within contact importance of the slow and fast reporting groups respectively, having subset them to the non-negligible age ranges (0-34 rather than 0-70+). The fact that the slow reporters are more important to the dynamics of an epidemic are more observable in this plot. See [7] for full numerical implementation.

This application highlights the importance of reporting infection quickly and effectively, as one can observe that the \mathcal{R}_0 was significantly more sensitive to the presence of the slower reporting group. From the results of Figure 7, we can see that the younger age ranges would be most responsible for a resulting epidemic; this could allow for more sophisticated epidemic-control measures, such as advertising specifically targeting the age ranges that are most responsible for the spread of the infection. In particular one would target children aged 5-9, perhaps by using social media to educate their parents or by the immediate closure of schools. In this section, we have

shown how the importance of particular types or contacts within a population can be analytically approximated through spectral methods. This work is particularly relevant to real world applications, as being able to identify and isolate the members of a population most responsible for a resulting epidemic could reduce its final size [22], and thus save lives.

6 Discussion and Further Work

In this report, we have looked at two ways in which heterogeneity may be introduced into the stochastic models, namely through time-dependent contact rates and the stratification of a population into heterogeneous groups. After giving a brief introduction to the basic stochastic SIR model and how it may be numerically simulated (Sections 2 and 3), we moved on to study how introducing heterogeneity altered the dynamics of a resulting epidemic. Namely, in Section 4, we presented a novel model that analytically approximated the probability of a major epidemic, based upon the time a single infective was introduced to the system. We applied our results to two examples motivated within literature, and in both cases we demonstrated that our model provides more accurate information than assuming a constant contact rate. In Section 5, we instead studied population heterogeneity and how we can separate a population into groups of different types. We then presented a novel application of results from network science, which we used to find which type in our population was most responsible for a resulting epidemic. Using real-contact data from the literature, we applied this theory to observe the effect slow reporting has on an epidemic, as motivated by the current work of Thompson [29]. Although we have presented some ways in which heterogeneity can be introduced into stochastic epidemic modelling, we have by no means given an exhaustive list. There are many ways in which stochastic epidemic models can be further generalised to be more applicable to real-world scenarios, for example one may want to consider a population which is not heterogeneously mixed. Such a model could be used for populations with cliques, where a disease is more likely to spread within a clique than between different cliques. To extent the ideas presented in this report, one could develop an analogous result to our multi-type model importance, given by (30), to the case where a contact structure exists in the population. We encourage an interested reader to view the corresponding Python notebooks for this report, which present the numerical implementations of all methods described [7].

Acknowledgement The author would like to thank their supervisor, Dr. Robin Thompson for his support and direction throughout the duration of this report. In addition to excellent project guidance, they found his discussions regarding the real-world applications of epidemiology to highlight the importance of mathematical research.

Word count: Approximately 7600, counted on OverLeaf (including appendices and excluding bibliography, table of contents, mathematical equations, diagrams and abstract).

References

- [1] Hannah Ritchie and Max Roser. Causes of Death. *Our World in Data*, 2020. <https://ourworldindata.org/causes-of-death>, [Online; accessed 23/04/2020].
- [2] Ronald Ross. Some a priori pathometric equations. *British Medical Journal*, 1(2830):546, 1915.
- [3] William Kermack and Anderson McKendrick. A contribution to the mathematical theory of epidemics. *Proceedings of the Royal Society of London. Series A, Containing papers of a Mathematical and Physical character*, 115(772):700–721, 1927.
- [4] Maurice S Bartlett. Deterministic and stochastic models for recurrent epidemics. In *Proceedings of the third Berkeley symposium on mathematical statistics and probability*, volume 4, page 109, 1956.
- [5] Norman TJ Bailey. A simple stochastic epidemic. *Biometrika*, pages 193–202, 1950.
- [6] Divine Wanduku. A comparative stochastic and deterministic study of a class of epidemic dynamic models for malaria: exploring the impacts of noise on eradication and persistence of disease. *arXiv preprint arXiv:1809.03897*, 2018.
- [7] Candidate Number: 1041671. *GitHub Repository: Heterogeneity in Stochastic Epidemic Models*, 2020. https://github.com/thomasarmstrong98/epidemic_modelling, [Online; accessed 30/04/2020].
- [8] James C Frauenthal. Deterministic epidemic models. In *Mathematical Modeling in Epidemiology*, pages 1–11. Springer, 1980.
- [9] Anderson, R. M. and May, R. *Infectious Diseases of Humans: Dynamics and Control*. Oxford University Press, 1991.
- [10] Vanja Dukic, Hedibert F Lopes, and Nicholas G Polson. Tracking epidemics with Google flu trends data and a state-space SEIR model. *Journal of the American Statistical Association*, 107(500):1410–1426, 2012.
- [11] P Whittle. The outcome of a stochastic epidemic—a note on bailey’s paper. *Biometrika*, 42(1-2):116–122, 1955.
- [12] Robin Thompson, Chris Gilligan, and Nik Cunniffe. When does a minor outbreak become a major epidemic? Linking the risk from invading pathogens to practical definitions of a major epidemic. *BioRxiv*, page 768853, 2019.

- [13] Linda JS Allen. Stochastic Population and Epidemic Models. *Mathematical Biosciences lecture series, Stochastics in Biological Systems*, 2015.
- [14] Helen Abbey. An examination of the Reed-Frost theory of epidemics. *Human Biology*, 24(3):201, 1952.
- [15] Christine Jacob. Branching processes: their role in epidemiology. *International journal of environmental research and public health*, 7(3):1186–1204, 2010.
- [16] Jesús R Artalejo, A Economou, and María Jesús Lopez-Herrero. Stochastic epidemic models revisited: analysis of some continuous performance measures. *Journal of biological dynamics*, 6(2):189–211, 2012.
- [17] Daniel T Gillespie. Exact stochastic simulation of coupled chemical reactions. *The journal of physical chemistry*, 81(25):2340–2361, 1977.
- [18] Ting Lu, Dmitri Volfson, Lev Tsimring, and Jeff Hasty. Cellular growth and division in the Gillespie algorithm. *Systems biology*, 1(1):121–128, 2004.
- [19] Eric Jones, Travis Oliphant, Pearu Peterson, et al. *SciPy: Open source scientific tools for Python*, 2001–. <http://www.scipy.org/>, [Online; accessed 23/04/2020].
- [20] Gerardo Chowell, Nick W Hengartner, Carlos Castillo-Chavez, Paul W Fenimore, and Jim Michael Hyman. The basic reproductive number of Ebola and the effects of public health measures: the cases of Congo and Uganda. *Journal of theoretical biology*, 229(1):119–126, 2004.
- [21] Dennis Mollison and Salah Ud Din. Deterministic and stochastic models for the seasonal variability of measles transmission. *Mathematical biosciences*, 117(1-2):155–177, 1993.
- [22] Aadrita Nandi and Linda JS Allen. Stochastic multigroup epidemic models: Duration and final size. In *Modeling, Stochastic Control, Optimization, and Applications*, pages 483–507. Springer, 2019.
- [23] Klaus Dietz and KP Haderler. Epidemiological models for sexually transmitted diseases. *Journal of mathematical biology*, 26(1):1–25, 1988.
- [24] Toshikazu Kuniya, Jinliang Wang, and Hisashi Inaba. A multi-group sir epidemic model with age structure. *Discrete & Continuous Dynamical Systems-B*, 21(10):3515, 2016.
- [25] Odo Diekmann, JAP Heesterbeek, and Michael G Roberts. The construction of next-generation matrices for compartmental epidemic models. *Journal of the Royal Society Interface*, 7(47):873–885, 2010.
- [26] Aadrita Nandi and Linda JS Allen. Stochastic two-group models with transmission dependent on host infectivity or susceptibility. *Journal of biological dynamics*, 13(sup1):201–224, 2019.

- [27] Juan G Restrepo, Edward Ott, and Brian R Hunt. Characterizing the dynamical importance of network nodes and links. *Physical review letters*, 97(9):094102, 2006.
- [28] James P Keener. The Perron–Frobenius theorem and the ranking of football teams. *SIAM review*, 35(1):80–93, 1993.
- [29] Robin N Thompson. Novel coronavirus outbreak in Wuhan, China, 2020: Intense surveillance Is vital for preventing sustained transmission in new locations. *Journal of clinical medicine*, 9(2):498, 2020.
- [30] Joël Mossong, Niel Hens, Mark Jit, Philippe Beutels, Kari Auranen, Rafael Mikolajczyk, Marco Massari, Stefania Salmaso, Gianpaolo Scalia Tomba, Jacco Wallinga, et al. Social contacts and mixing patterns relevant to the spread of infectious diseases. *PLoS medicine*, 5(3), 2008.

Appendix A

In this section, we derive (10) for how the probability of an epidemic changes based upon its infective introduction time. We start by factorising and simplifying (9), with the substitution $u = 1 - q$, to obtain

$$\frac{du}{dt} + u(B(t) - \gamma) = B(t)u^2$$

which is of Bernoulli's form. Further substituting with $v = u^{-1}$, we have that

$$\frac{dv}{dt} - v(B(t) - \gamma) = -B(t).$$

This is a simple first order ODE which can be solved using the integrating factor $IF = \exp\{-\int B(t') - \gamma dt'\}$, to obtain

$$v(t) = \frac{C - \int^t B(t') \exp\{-\int^{t'} B(\tau) - \gamma d\tau\} dt'}{\exp\{-\int^t B(t') - \gamma dt'\}} \quad (31)$$

where C is an integration constant. By back-substituting to find q , we obtain the probability of no major epidemic, given that an infective was introduced at time \bar{t} as

$$q(\bar{t}) = 1 - \frac{\exp\{-\int^{\bar{t}} B(t') - \gamma dt'\}}{C - \int^{\bar{t}} B(t') \exp\{-\int^{t'} B(\tau) - \gamma d\tau\} dt'}. \quad (32)$$

As described in the main text, we can therefore consider the probability of a resulting major epidemic $p(\bar{t})$ by taking $1 - q(\bar{t})$. The initial condition for (32) can be found through numerical simulation, or by assuming properties of the function (for example if it is periodic).

Appendix B

In this section, we derive the equations, (30), for the dynamical importance of the infectious type and contact, by using the methods explained in [27]. The full derivation of infectious type, which we now provide, was omitted from the original paper. First, we consider the next-generation matrix \mathbf{K} of the multi-type SIR model defined by Table 1.

$$\mathbf{K} = \begin{bmatrix} \frac{B_{11}}{\gamma_1} & \frac{B_{12}}{\gamma_2} & \cdots & \frac{B_{1M}}{\gamma_M} \\ \vdots & & \ddots & \vdots \\ \frac{B_{M1}}{\gamma_1} & \cdots & & \frac{B_{MM}}{\gamma_M} \end{bmatrix}. \quad (33)$$

Infectious Type Importance

As described in Section 5, we want to find $\Delta\lambda_k$, which is the difference between the largest eigenvalue of \mathbf{K} and the largest eigenvalue of a next generation for a system in which type k has been removed. To construct the altered next generation matrix, we consider a matrix

$$\hat{\mathbf{K}} = \mathbf{K} + \Delta\mathbf{K}, \quad (34)$$

where the matrix $\hat{\mathbf{K}}$ is the next generation matrix of the new system (the k^{th} row and column has been removed of \mathbf{K} have been removed). The matrix $\Delta\mathbf{K}$ therefore takes the form

$$(\Delta\mathbf{K})_{i,j} = -K_{i,j}(\delta_{i,k} + \delta_{k,j} - \delta_{i,k}\delta_{i,j}). \quad (35)$$

where $\delta_{i,j}$ is the Kronecker Delta. If we let $\hat{\mathbf{u}} = \mathbf{u} + \Delta\mathbf{u}$ be the corresponding right eigenvector of the altered next generation with eigenvalue $\hat{\lambda} = \lambda + \Delta\lambda_k$, then we have that

$$\begin{aligned} \hat{\mathbf{K}}\hat{\mathbf{u}} &= \hat{\lambda}\hat{\mathbf{u}}, \text{ which can also be written as} \\ (\mathbf{K} + \Delta\mathbf{K}_k)(\mathbf{u} + \Delta\mathbf{u}) &= (\lambda + \Delta\lambda_k)(\mathbf{u} + \Delta\mathbf{u}) \end{aligned} \quad (36)$$

Since we have removed the the k^{th} row of \mathbf{K} by setting all entries to zero, the corresponding k^{th} entry of the eigenvector $\hat{\mathbf{u}}$ will also be zero. We therefore re-write the term $\Delta\mathbf{u}$ as

$$\Delta\mathbf{u} = \delta\mathbf{u} - \mathbf{u}\mathbf{e}_k. \quad (37)$$

By left multiplying (36) by the left eigenvector \mathbf{v} and expanding out the brackets, we obtain the following

$$\Delta\lambda_k = \frac{\mathbf{v}^T \Delta \mathbf{K} \mathbf{u} - u_k \mathbf{v}^T \Delta \mathbf{K} \mathbf{e}_k}{\mathbf{v}^T \mathbf{u} - v_k u_k} \quad (38)$$

where the second order terms $\mathbf{v}^T \Delta K \delta \mathbf{u}$ and $\Delta \lambda \mathbf{v}^T \delta \mathbf{u}$ have been neglected. The ignoring of these terms is dubious, but when the number of types we consider are sufficiently large, these terms become small enough to neglect. We will now consider the numerator term-by-term and show how they approximate the desired result given by (28). The first term, $\mathbf{v}^T \Delta \mathbf{K} \mathbf{u}$, takes the following form

$$\mathbf{v}^T \Delta \mathbf{K} \mathbf{u} = [v_1, \dots, v_n] \begin{bmatrix} & & -\frac{B_{1,k}}{\gamma_k} & & \\ & & \vdots & & \\ -\frac{B_{k,1}}{\gamma_1} & \dots & -\frac{B_{k,k}}{\gamma_k} & \dots & -\frac{B_{k,M}}{\gamma_M} \\ & & \vdots & & \\ & & -\frac{B_{M,k}}{\gamma_k} & & \end{bmatrix} \begin{bmatrix} u_1 \\ u_2 \\ \vdots \\ u_M \end{bmatrix}.$$

By considering the entry-wise multiplication of the matrix-vector products, we obtain

$$\mathbf{v}^T \Delta \mathbf{K} \mathbf{u} = -\frac{u_k}{\gamma_k} \sum_{\substack{l=1 \\ l \neq k}}^M B_{l,k} v_l - v_k \underbrace{\sum_{i=1}^M \frac{B_{k,i}}{\gamma_i} u_i}_{= \lambda u_k}.$$

Simplifying the above gives

$$\mathbf{v}^T \Delta \mathbf{K} \mathbf{u} = -u_k \underbrace{\sum_{\substack{l=1 \\ l \neq k}}^M \frac{B_{i,k} v_l}{\gamma_k}}_{\approx \lambda u_k} - \lambda u_k v_k, \text{ which leads to} \quad (39)$$

$$= -2\lambda u_k v_k. \quad (40)$$

Likewise, we can consider the second term $\mathbf{u}_k \mathbf{v}^T \Delta \mathbf{K} \mathbf{e}_k$; in a similar vein to the term we just simplified, $\mathbf{u}_k \mathbf{v}^T \Delta \mathbf{K} \mathbf{e}_k$ can be written as

$$\begin{aligned} \mathbf{u}_k \mathbf{v}^T \Delta \mathbf{K} \mathbf{e}_k &= -u_k \sum_{i=1}^M \frac{B_{i,k}}{\gamma_k} v_i \\ &= -\lambda u_k v_k. \end{aligned}$$

By re-writing (36) using the simplified (and approximated) terms, we have that

$$\Delta\lambda_k = -\frac{\lambda u_k v_k}{\mathbf{v}^T \mathbf{u} - u_k v_k}. \quad (41)$$

The infectious type importance for a type k is therefore

$$\hat{\mathcal{I}}_k = \frac{u_k v_k}{\mathbf{v}^T \mathbf{u} - u_k v_k} \quad \text{as required.}$$

Contact Importance

For brevity, the derivation for the contact rate formula is omitted, however it is almost identical to that of the infectious type derivation except that the term $\Delta\mathbf{u}$ does not need to be re-written as it is sufficiently small that it may be neglected in second order terms. By considering similar methods and approximations to those used previously, we obtain that the contact importance for between an infectious of type j to a susceptible of type i is given by

$$\hat{\mathcal{I}}_{i,j} = \frac{K_{i,j} v_i u_j}{\lambda \mathbf{v}^T \mathbf{u}}.$$

For more information, the reader is directed to the paper by [27], where they construct an analogous result for node and edge importance on networks.